The Meteoritical Society

Meteoritics & Planetary Science 44, Nr 1, 43–54 (2009)
Abstract available online at http://meteoritics.org

Layered ejecta craters and the early water/ice aquifer on Mars

Verne R. OBERBECK

NASA Retired, 5650 24th Ave. NW #503, Seattle, Washington 98107, USA
*Corresponding author. E-mail: verne.oberbeck@yahoo.com

(Received 14 January 2008; revision accepted 17 July 2008)

Abstract–A model for emplacement of deposits of impact craters is presented that explains the size range of Martian layered ejecta craters between 5 km and 60 km in diameter in the low and middle latitudes. The impact model provides estimates of the water content of crater deposits relative to volatile content in the aquifer of Mars. These estimates together with the amount of water required to initiate fluid flow in terrestrial debris flows provide an estimate of 21% by volume (7.6×10^7 km^3) of water/ice that was stored between 0.27 and 2.5 km depth in the crust of Mars during Hesperian and Amazonian time. This would have been sufficient to supply the water for an ocean in the northern lowlands of Mars. The existence of fluidized craters smaller than 5 km diameter in some places on Mars suggests that volatiles were present locally at depths less than 0.27 km. Deposits of Martian craters may be ideal sites for searches for fossils of early organisms that may have existed in the water table if life originated on Mars.

INTRODUCTION

Many geomorphic studies of Martian layered ejecta craters have been made. Most of the early workers concluded that ice/water caused fluid like flow in crater deposits (Head and Roth 1976; Carr 1977; Carr et al. 1977; Gault and Greeley 1978; Mouginis-Mark 1981; Greeley et al. 1980; Barlow and Bradley 1990). Later, Schultz and Gault (1979) and Schultz (1992) proposed that fine ejecta was winnowed from the ejecta curtain by atmospheric deceleration, suspended in winds generated by vortices, and deposited after ballistic emplacement of ejecta. Barnouin-Jha and Schultz (1998) and Barnouin-Jha et al. (1999) also studied this mechanism. Boyce and Mouginis-Mark (2006) proposed that vortices from atmospheric interactions or base surges may have eroded inner layers and deposited material in the outer layers of double layer ejecta craters (DLE). McSaveney and Davies (2005) proposed that gases and inter-grain gliding could have produced fluid flow of deposits. Ivanov (1996) used a Bingham flow model to show that Bingham parameters for deposit emplacement fell between those that are characteristic of dry rock avalanches and volatile rich debris flows. The model ratios of the deposit radii to crater radii were found to depend on scale even for constant volatile content (Ivanov and Pogoretsky 1996) suggesting that fluidization does not depend on volatiles alone. Barnouin-Jha et al. (2005) and Barnouin-Jha and Buczkowski (2007) provided a model of ejecta runout that gave runout distances for crater deposits that were similar to those of terrestrial dry rock avalanche deposits, Martian landslides, and dry volcanic flow deposits if it was assumed that impacting ejecta was well separated. Runout distances were similar to those of volatile rich terrestrial debris flows for assumed ejecta impact between single body and well-separated ejecta impacts.

The large numbers of mechanisms that have been proposed to fluidize crater deposits suggest the need for a renewed critical evaluation of the role that volatiles may have played in fluidizing deposits. It is the purpose of this paper to use an impact model for emplacement of crater deposits to determine whether crustal volatiles could have produced the observed size distributions of craters with layered deposits.

A MODEL FOR EMPLACEMENT OF MARTIAN FLUIDIZED DEPOSITS

The solid lines in Fig. 1a represent streamlines of excavation for ejecta exiting at radius r_c from the center of a growing impact crater. The percentage of volatiles in ejecta at A and B and in this ejecta when it impacts around an impact crater (Fig. 1b.) depends on the percentage of the crater excavation streamline exiting at r_c that traverses the aquifer, the percentage of volatiles in the aquifer, and the amount of volatiles added from ballistic erosion during ejecta impact outside the crater. Ejecta impacting around the crater can mix surface material into the crater ejecta if impact velocity is high enough (Oberbeck 1975). In Fig.1b,

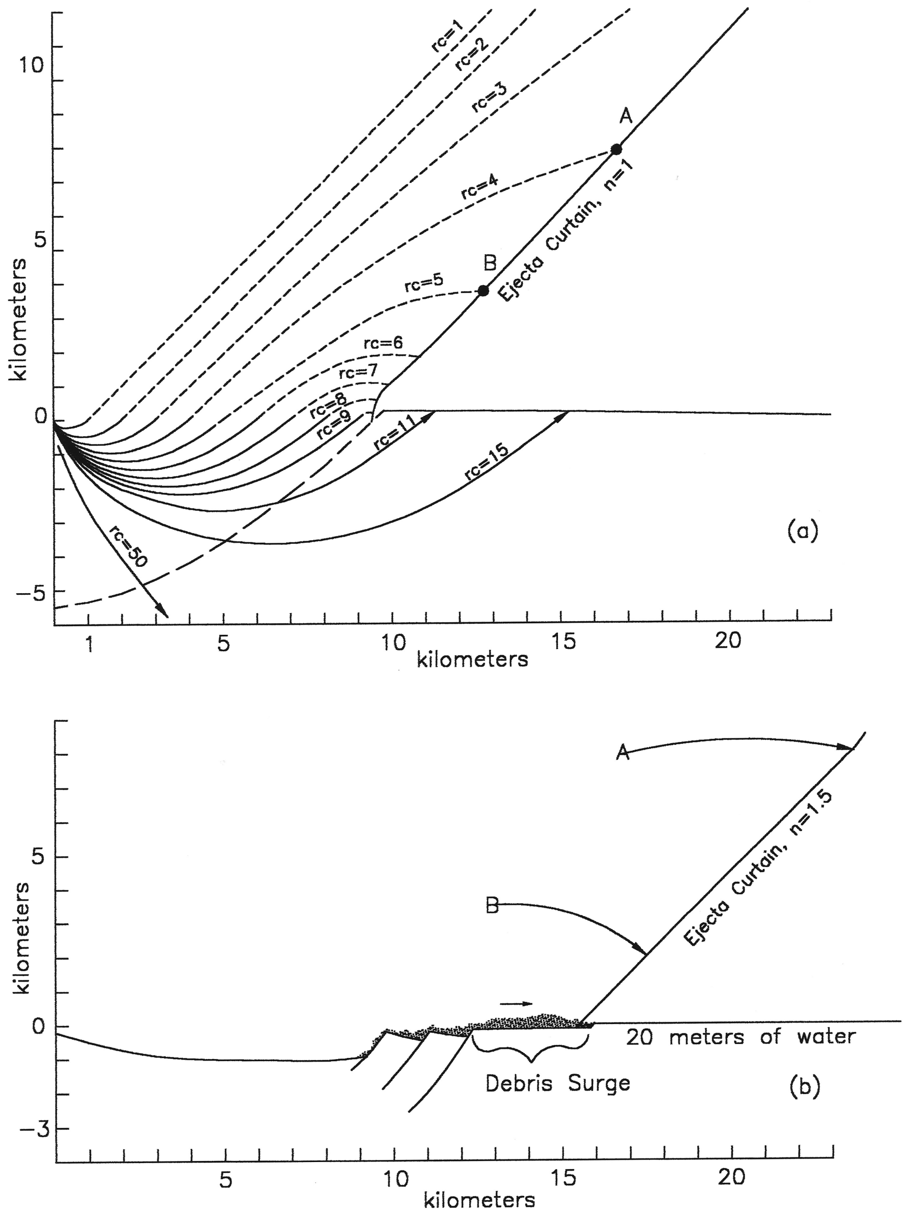

Fig. 1. a) Solid lines are streamlines for excavation of ejecta launched at various radii r_c in crater of excavation. Dotted lines are ballistic trajectories of ejecta containing volatiles from the crust. Ejecta curtain is at the location when the transient crater has formed and A and B show positions of ejecta at that time in the ejecta curtain. b) Ejecta curtain has moved away from the crater rim, the crater has collapsed and the ground surge of fluidized ejecta and eroded material containing surface volatiles has flowed along the ground behind the ejecta curtain.

a 20-meter depth of water is shown at the surface outside the crater. This figure depicts emplacement of crater ejecta on a surface water environment on Earth. Ballistic erosion at the base of the ejecta curtain incorporates surface water and sediments into the deposit and adds it to water and crustal material from the primary crater. A ground surge of fluidized ejecta and ballistic erosion material moves out behind the ejecta curtain as in Fig. 1b. If surface volatiles are absent, as on planets like Mars that lack appreciable atmospheres, ballistic erosion outside the crater would mix volatile poor surface material into the crater deposits and dilute volatiles coming from the primary crater of excavation. Thus, in order to determine volatile content of Martian crater deposits, streamlines of crater excavation at r_c must be defined and launch velocities for each streamline must be determined to find the percentage of volatiles in ejecta, the range of deposition of primary crater volatiles, and the amount of ballistic erosion at any point in the deposit.

Streamlines corresponding to each radius of launch r_c are obtained by using the following equation for streamlines taken from the Z model (Croft 1980):

$$R_s = r_c(1 - \cos\theta) \quad (1)$$

where θ is the angle of the streamline in polar coordinates and R_s and θ define the path of the streamline for material being excavated from the crater at r_c. Equation 1 applies when Z in the Z model is 3 and the origin of streamlines is at the surface. It was used in this study to find the percentage of the streamline below a given volatile table depth. For streamlines of excavations following Equation 1, Fig. 2 shows a plot that gives the percentage of a streamline that is below the depth h of a volatile table expressed as a function of h/ r_c. For example, a streamline exiting at r_c = 10 km where the volatile table is h = 1 km is characterized by h/ r_c = 0.1. From Fig. 2, 77% of the streamline exiting at 10 km is from below the 1 km volatile table. If the aquifer does not extend to the maximum excavation depth of a given streamline, the percentage of the streamline below the lower boundary of the aquifer is determined and subtracted from the percentage below the upper boundary to find the percentage of the streamline within the aquifer. The percentage of the streamline within the aquifer as determined from Fig. 2 is then equated to X_p, the percentage of primary crater ejecta from r_c that contains volatiles. This is needed later to compute water/ice content at specific locations in crater deposits. Next, the velocity of launch, V, of material ejected from each streamline at r_c is needed for calculation of range of transport of material launched at each r_c so that X_p determined for each streamline can be used to compute volatile content at specific locations in crater deposits.

Melosh (1989) adopted the following ejecta scaling relationship of Housen et al. (1983) for the velocity of ejection for material ejected from the excavation streamlines at radius r_c within a growing crater of final transient radius R when gravity controls crater growth as for the crater sizes considered here:

$$V = k(r_c/R)^{-1.8}(gR)^{0.5} \quad (2)$$

g is the acceleration of gravity. Melosh (1989) assumed k equal to 0.4 and −1.8 for the exponent, the values assumed here. 0.4 is the equal to the average value for k found in experiments performed later by Cintala et al. (1999). −1.8 is near the average for the values of −1.5, −1.8, and −2.4 for impact in basalt, water, and quartz sand targets (Housen et al.1983).

From V, the range of ejecta transport beyond r_c is obtained from the classic ballistic equation:

$$r_t = V^2 \mathrm{Sin}\ 2\psi/g \quad (3)$$

where ψ is ejection angle = 45 degrees when Z = 3 is assumed in the Z model. Substitution of V from Equation 2 into Equation 3, letting ψ equal 45 degrees and simplifying, gives r_t for material launched at r_c for a crater of transient radius R:

$$r_t = 0.16(r_c)^{-3.6}R^{4.6} \quad (4)$$

It is assumed in this substitution of V that there is no deceleration of material in the ejecta curtain depositing material between R and 2 R because in this region the ejecta curtain is continuous and would not be slowed by the atmosphere even if present. In addition, this close to impact the atmosphere would already have been pushed aside by the impact vapor plume that advanced in front of the thick ejecta curtain.

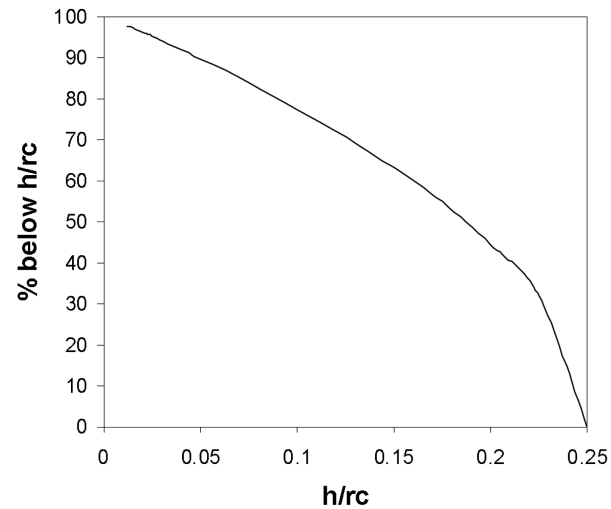

Fig. 2. Percent of streamline of excavation beneath depth h in the crust plotted against the ratio h/r_c.

Substituting Equation 4 for r_t in the following equation, the range r from the center of a transient crater of radius R of ejecta that is launched at r_c is:

$$r = r_c + r_t = r_c + 0.16r_c^{-3.6} R^{4.6}. \quad (5)$$

For craters that are small enough to eject material at low enough velocities that deposits are emplaced at r without ballistic erosion of the surrounding surface materials, no mixing of primary crater ejecta with surface material outside the crater occurs. The percentage of ice/water in the ejecta, β, impacting at r is:

$$\beta = (\Omega/100)\ [\ X_p\ ] \quad (6)$$

where X_p is the percentage of the primary crater ejecta that is from the aquifer (percent of the streamline exiting at r_c that is in the aquifer and that is transported to r) and Ω is the percentage of volatiles in the aquifer. For example, if 50% of the primary ejecta in a streamline at r_c is material from the aquifer (X_p = 50%) and if 50% of the material in the aquifer is volatile material (Ω = 50%), that part of the ejecta impacting at r (Equation 5) from this streamline would contain 25% volatiles (Equation 6). The ratio of deposit volatile content and aquifer volatile content for ejecta impacting at the computed location r (Equation 5) in the deposit is:

$$\beta/\Omega = X_p/100. \quad (7)$$

This ratio is convenient for determining which crater sizes have deposits with higher volatile content relative to the aquifer volatile content. It can also be used to calculate the aquifer ice/water content Ω required to fluidize any part of a crater deposit if the volatile content required to initiate fluid flow in debris flows, β, is known.

For sufficiently large impact craters, primary crater ejecta erodes near surface material when it impacts outside the crater (Oberbeck 1975). This can either add volatiles or dry material to crater deposits dependent on whether volatiles are excavated by ballistic erosion when ejecta impacts outside the crater. Oberbeck (1975) defined the parameter μ as the ratio of ballistic erosion mass and primary crater ejecta mass as a measure of the amount of ballistic erosion. The amount of ballistic erosion in soil or competent rock can also be derived from a cratering efficiency Equation (ratio of crater displaced mass to projectile mass) given for single body impacts when crater growth is controlled by gravity (Melosh (1989):

$$\pi_v = 0.2(1.61gL/ V^2)^{-0.65}. \quad (8a)$$

This is taken to be appropriate for a regolith on a megaregolith of formations shattered by impact. L is the size of the projectile and V is impact velocity. L is taken here as the thickness of the ejecta at the base of the ejecta curtain at r and V is the ejection/impact velocity of ejecta impacting at r of material launched at r_c. For efficiency ratios up to five, which are not exceeded in this study, values assumed for single body impact are appropriate for impacting crater ejecta (Petro and Pieters 2006). π_v is reduced by one fourth the value given in Equation 8a because ejected mass is one fourth displaced mass. Ballistic erosion efficiency is thus one fourth the value given by Equation 8a:

$$\mu = .036(gL/ V^2)^{-0.65} \quad (8b)$$

where V (from Equation 2) is the ejection/impact velocity of material launched at r_c to range r (Equation 5), and where ejecta thickness is L:

$$L = 0.12R^{0.74}(r/R)^{-2.9} \quad (9a)$$

$$L = 0.02R^{0.74}(r/R)^{-2.9}. \quad (9b)$$

Equation 9a is for decay of ejecta thickness around an impact crater, where R is transient crater radius when dimensions are given in meters. I use the exponent −2.9 and the constant 0.12 rather than the exponent −3.0 and the constant 0.14 used by McGetchin et al. (1977) because I find that these values provides ejecta volumes more in agreement with excavation volumes predicted using the Z model for impact crater ejection (Croft 1980). Equation 9b is expressed in km.

In order to check the validity of Equation 8b, let us compare μ, the ratio of local ballistic erosion volume and primary crater ejecta volume derived from the core measurements in the deposit of the Ries crater (Hörz et al. 1977, 1983) to μ values given by Equation 8b. An ancient pre-impact marine cliff line occurs at about 16.5 km from the Ries crater impact point within the deposit area. Ballistic erosion excavated fossils from the cliff line and carried them as little as 2 km and as much 10 km outward in the debris ground surge (Hörz et al. 1977). Thus a μ value for ejecta impacting at 16.5 km may be calculated and compared with μ values observed in cores found at average range r = 21.5 km. A thickness of .028 km of primary ejecta L was determined at 16.5 km from Equation 9b and transient radius =10.2 km for the Ries crater. V for material impacting at 16.5 km was determined to be 320 m/s from Equation 2 and r_c = 6.1 km, the value corresponding to r= 16.5 km as given by Equation 5. L and V are then substituted into Equation 8b to give μ = 1.7. A core value of μ = 1.5 can be interpolated at 21.5 km in deposits of the Ries crater from cores measurements of erosion products at various radii in the Ries deposit (Hörz et al. 1977, 1983) summarized in Morrison and Oberbeck (1978). This agreement between core measurements of ballistic erosion and model calculations validates use of Equation 8b for calculating ballistic erosion efficiency.

The percentage, by volume, β, of water in deposits of impact craters that emplace deposits with ballistic erosion of pre-existing ground around the primary crater, can be expressed in terms of the volume of volatiles present in both the primary ejecta and secondary ballistic erosion material, both of which are given within the brackets in the numerator of Equation 10 and the total volume of primary ejecta and secondary erosion volume given in the denominator of Equation 10:

$$\beta = 100[(\Omega/100)(X_p/100)V_p + (\Omega/100)(X_s/100)V_s] \{V_p + V_s\}^{-1} \quad (10)$$

where is Ω the percent of volatiles in the aquifer, X_p is the percent of the primary ejecta that is derived from within the aquifer, X_s is the percent of secondary ballistically eroded material that is derived from within the aquifer, V_p is the volume of the primary ejecta and V_s is the volume of secondary ballistically eroded material in the deposit. X_s is determined from the percentage of total excavation depth from ballistic erosion that is in the aquifer:

$$X_s = \{\mu\ L\text{- (depth of aquifer)}/\mu\ L\}100. \quad (11)$$

For 0 or negative values $X_s = 0$. Given that ejecta density and ballistic erosion material are the same, $V_s = \mu V_p$, and Equation 10 can be reduced to Equation 12:

$$\beta = (\Omega /100)\ [X_p + X_s\ \mu]\ \{1 + \mu\}^{-1}. \quad (12)$$

As a sample calculation assume that 50% of the crust within the aquifer is volatiles (Ω = 50%). Assume that 50% of the primary crater ejecta is material from within the aquifer (X_p = 50%). If so, primary ejecta contains 25% volatiles. Assume also that 25% of the ballistic erosion volume is material from within the aquifer (X_s = 25%). Then ballistic erosion material contains 12.5% volatiles. Finally, assume that there is twice the amount of secondary ballistic erosion material in the deposit as primary ejecta (μ = 2). The primary and secondary ejecta combined as the deposit would then contain two parts ballistic erosion material and one part primary crater ejecta and 16.6% ice/water since there is twice as much ballistic erosion material as primary crater ejecta. It is seen that Equation 12 gives the correct answer of 16.6% for β because 16.6% is obtained by substitution of the values in the parentheses above into Equation 12. Equation 12 reduces to Equation 7 for deposit emplacement with no ballistic erosion if $\mu = 0$ is substituted into Equation 12. Equation 13 gives the ratio of percent volatiles in the deposit and percent volatiles in the aquifer:

$$\beta/\Omega = (100)^{-1}\,[X_p + X_s\,\mu]\,\{1 + \mu\}^{-1}. \qquad (13)$$

For deposits of craters of the size considered in this study (up to 166 km), ballistic erosion depth is less than 0.27 km. Therefore, X_s in Equation 13 is 0 for all cases because the absence of layered ejecta craters less than 5 km means that the upper 0.27 km of the crust is volatile free. None of the ballistic erosion material would therefore contain volatiles. Equation 13 simplifies to:

$$\beta/\Omega = (100)^{-1}\,[X_p]\,\{1 + \mu\}^{-1}. \qquad (14)$$

Thus, at any given position in the deposits of a crater, either Equation 7 or Equation 14 was used with X_p and μ to determine (β/Ω), the volatile content of the deposit relative to aquifer volatile content. Selection of which equation that was used depended on whether the velocity of impact of the ejecta at r exceeded the velocity to cause ballistic erosion. If it did, Equation 14 was used and if it did not Equation 7 was used. Morrison and Oberbeck (1978) found velocities of 200–300 meters per second formed subdued secondary craters in the regolith-mare basalt surface beneath the continuous deposits of 25.5 km diameter lunar crater Delisle. At 16.5 km range from impact point at the Ries crater, impact velocity in weakly bonded surface sand was 320 meters per second. I found μ to be 1.7 for deposit material set in motion at this range, in agreement with observed values at final position of deposition. Beyond 16.5 km from impact and 320 meters per second emplacement velocity, μ increases rapidly. Emplacement of ejecta on regolith-competent targets on the Moon and weakly bonded material resting on competent rock on Earth suggest that 320 meters per second may be taken as that velocity required for onset of significant ballistic erosion during impact of primary ejecta in the region of the continuous deposits of impact craters formed in mixtures of regolith and shattered and competent rock on Mars. Thus, for ejecta impacting from streamlines that ejected material at velocities greater than 320 m/s, Equation 14 was used to calculate β/Ω for crater deposits.

RESULTS

A catalog of Martian layered ejecta craters produced by Barlow and Bradley (1990) shows that most of the double layered ejecta craters (DLE) are less than 25 km. Most of the single layered ejecta craters (SLE) are also less than 25 km but some occur up to 54.5 km within 35 degrees from the equator and up to 66.5 km within 45 degrees latitude from the equator. Multiple layered ejecta craters (MLE) craters are mostly 25 km to 50km in diameter. Kuzmin et al. (1988) report a minimum (onset) diameter between 4–7 km diameter for layered ejecta craters in most regions of the low and middle latitudes of Mars. Thus, a range of 5 to 60 km is adopted here as the size range of layered ejecta craters in most regions of the low and middle latitudes of Mars. The model will determine whether there is any distribution of volatiles in the crust of Mars that produces fluidized deposits of 5 to 60 km craters and non-fluidized deposits of craters smaller than 5 km and larger than 60 km diameter.

Equation 5 can be used to show that material ejected at the same ratio of r_c/R is transported in ballistic trajectories to the same ratios of r/R for any transient crater size R. Integration of Equation 2 of (Ivanov 1996) for Z model ejecta volume shows that 84% of crater ejecta is excavated from between $r_c = 0.54R$ and R. Substituting 0.54R for r_c in Equation 5 shows that 84% of crater ejecta impacts between R and 2R. After impact this material moves in a ground surge (Oberbeck 1975), to form the final continuous deposit. Therefore, the volatile content of material impacting between R and 2R and of material eroded by ejecta impacting in this region is of interest in determining the effect of ice/water on the nature of flow producing the continuous deposits of Martian layered ejecta craters. Ice/water content in ejecta and erosion material between R and 2R will be determined for deposits of many test craters of different size.

Test craters of 2.4 km, 3.2 km, 6 km, 9 km, 19 km, 38 km, 44 km, 60 km, and 100 km transient craters were used in the calculations. This range in crater size corresponds to final crater diameters of 3 km, 4 km, 7.5 km, 11 km, 25 km, 55 km, 65 km, 93 km, and 166 km, respectively. For craters less than or equal to 6 km, final diameter is 1.25 times transient diameter. For larger craters, the following relationship of Collins et al. (2005) is used:

$$D_f = .91\ D_t^{1.13}. \qquad (15)$$

Test craters with transient diameters listed above will be used to compute ice/water composition in deposits. Results in this section will be presented graphically for final diameters.

Because craters smaller than 5 km (4 km transient craters) lack fluidized deposits in most regions of the low and middle latitudes and because most of the ejecta in the deposit comes from 270 m depth, volatiles appear to have been absent in the upper <270 m of the crust. Because of this, and because the largest of the layered ejecta craters excavates at most less than 5 km depth, a aquifer extending from 270 meters to 5 km depth is a reasonable starting candidate for a aquifer that might produce the size range of layered and non-layered ejecta craters. It will be the first aquifer tested. The volatile

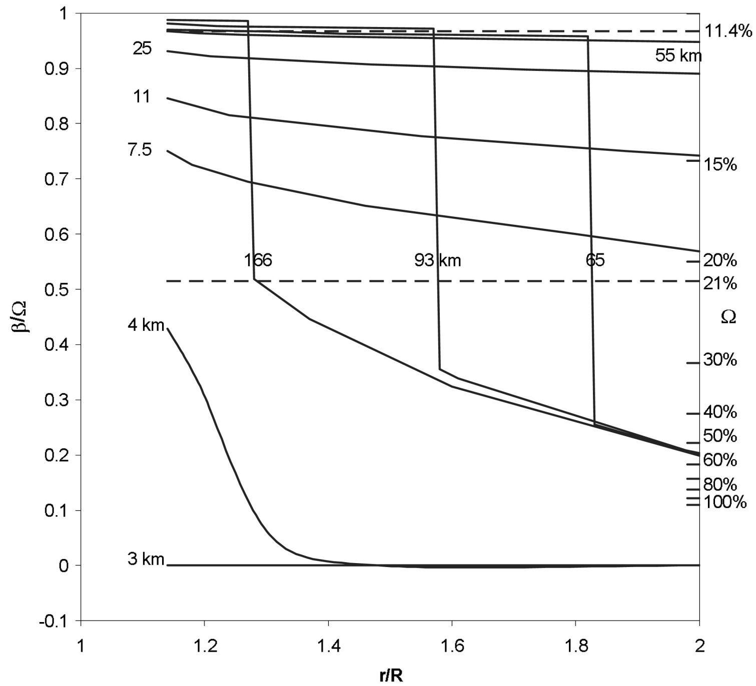

Fig. 3. For assumed volatiles between 0.27 and 5 km, the graphs show the ratio of percent volatiles in deposits and percent volatiles in the crust (β/Ω) at r/R in deposits (left Y axis) and percent volatiles in the crust (Ω) necessary to fluidized deposits at r/R for craters between 3 and 166 km diameter, assuming 11% volatiles are required for debris fluid flow (right Y axis).

content in ejecta impacting between 1.1 and 2 multiples of transient crater radius was computed for values of r_c, between .82R and .54R that propel material to these ranges. The percentage of each streamline that traversed within the aquifer (h = 0.27–5 km) was determined for each r_c value using the values used to prepare Fig. 2 for each crater and it was equated to X_p. The range r in the deposit was then calculated from r_c (Equation 5) for each packet of ejecta launched at r_c. X_p was then used with Equation 7 to determine the ratio β/Ω for each location in the deposits of craters whose deposits were emplaced at velocity less than 320 m/s. For those parts of deposits where ejecta impact velocity was greater than 320 m/s, L was obtained from Equation 9b for each r value and V was computed from Equation 2 for each r_c and corresponding r value. μ values for each r were computed from Equation 8b using L and V for each r. β/Ω ratios at each range were then calculated from Equation 14 using these μ and X_p values.

Figure 3 shows the ratios, β/Ω, for deposits of all crater sizes when volatiles are present between 270 meters and 5 km. The ratios of deposit ice/water content and aquifer volatile content of deposits of 7.5 to 55 km craters and deposits of 93 km and 65 km craters out to 1.6R and 1.8R, respectively, are greater than 0.55, whereas they are less than 0.55 for deposits of 3 km, 4 km, and 166 km craters and for distal portions of impacting ejecta of 93 km and 65 km crater deposits. The ratios are greater for 65 km and 93 km crater deposits than for 7.5 km and 55 km crater deposits. For any aquifer volatile content, the volatile content of 65 km and 93 km deposits out to 1.6R–1.8R would have been greater than the volatile content of the deposits of 7.5 km to 55 km craters. Since deposits of 7.5 to 55 km craters are fluidized and those of 65 km and 93 km craters are not, an aquifer extending from 270 meters to 5 km depth is not possible. An aquifer between 270 meters and 3.5 km is also not likely because the β/Ω ratios for deposits of 65 km craters are similar to those of layered ejecta craters less than 60 km but deposits of 65 km diameter craters are not fluidized in the low and middle latitudes.

Figure 4 shows the ratio of deposit volatile percent and percent volatiles in the aquifer, β/Ω, for deposits of 3 to 166 km craters when volatiles are present between 270 meters and 1.5 km. Deposits of 3 km and 4 km craters and deposits of craters between 65 and 166 km have β/Ω ratios less than 0.24 and deposits of craters between 7.5 km and 55 km have ratios greater than 0.24. For any aquifer volatile content, deposits of 7.5 km to 55 km craters will have higher volatile content than deposits of craters less than 5 km and larger than 60 km. This implies that this aquifer could have produced the observed size distribution of layered ejecta craters. However, the aquifer volatile content required to fluidize the crater deposits from such a thin aquifer is not consistent with the porosity of the Martian crust.

It is possible that during Hesperian time, the volatile could have contained liquid water that may have been ejected from the craters. However, some or all of the volatiles could have been ice. Stewart and Ahrens (2003) found that impact pressure converted 50% of the ground ice to liquid water in

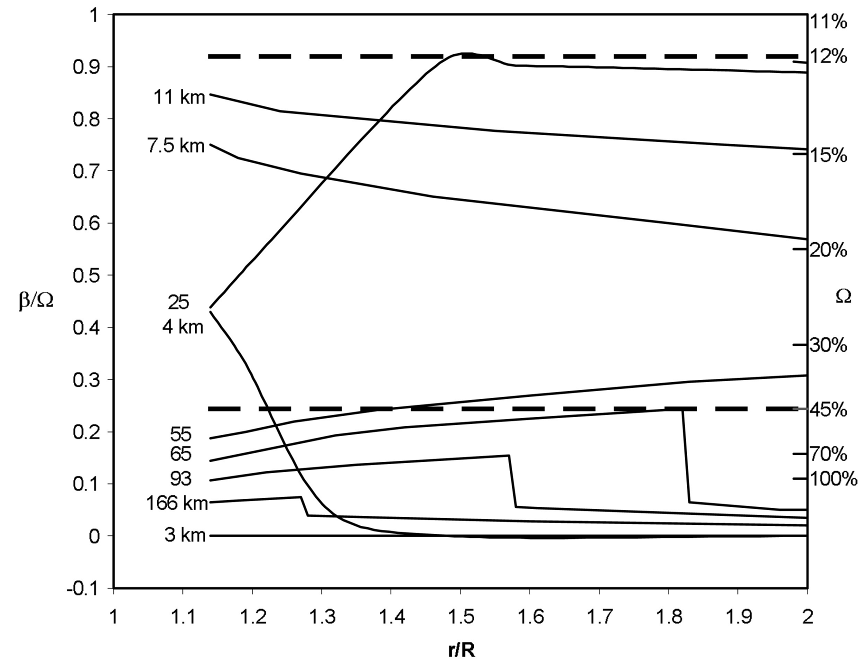

Fig 4. For assumed volatiles between 0.27 km and 1.5 km, the graphs show the ratio of percent volatiles in deposits and percent volatiles in the crust (β/Ω) at r/R in deposits (Left Y axis) and percent volatiles in the crust (Ω) necessary to fluidized deposits at r/R for craters between 3 km and 166 km diameter assuming 11% volatiles are required to fluidize crater deposits (Right Y axis).

primary crater ejecta and concluded that it would not have been necessary for volatiles in the crust to be liquid water to be able to fluidize crater deposits. Because all streamlines cross isobars, all streamlines would have contained liquid water that would have been mixed with ejecta. If volatiles in the ground surge was partly ice, ice at grain boundaries with silicates in the ground surge could also have been liquefied during turbulent high speed ground flow because pressure at grain contacts could have been sufficient to convert thin films of ice at contacts to water. Fink et al. (1981) concluded that terrestrial debris flows are analogs for Martian ejecta slurries and that 11% or more by volume of water in Martian crater deposits could prevented grain locking and would have imparted fluid flow to crater deposits if there is a wide assortment of particle sizes in debris (Rodine and Johnson 1976) as in impact ejecta. Pierson (1980) pointed out that even water contents as low as 10% impart flow of terrestrial debris on slopes as low as 8 degrees. Assuming 11% water/ice was required to fluidize deposits, β/Ω ratios in Fig. 4 may be used, with β = 11% to calculate Ω at each range r/R that would have been needed to fluidized deposits. This shows that Ω = 12% to 45% volatiles in the aquifer (the range on the right Y axis between the dotted lines in Fig. 4) would fluidize deposits of 7.5 to 55 km craters but not those of craters less than 5 km and greater than 60 km in diameter. However, the porosity of the Martian crust between 0.24 km and 1.5 km would have been insufficient to accommodate the 45% volatiles in the aquifer that would have been required to fluidize most of the deposits of 55 km diameter craters.

Clifford (1987) assumed a maximum surface porosity of 50% for a highly weathered megaregolith on Mars and used the following relationship for the decrease in porosity with depth, D, in the crust of Mars:

$$\phi(z) = \phi(0)\exp(-D/2.82) \qquad (16)$$

where $\phi(0)$ is the porosity at the surface. Assuming the maximum surface porosity of 50%, Equation 16 gives a maximum porosity at 1.5 km depth of 29 %. Averaging over the surface to 1.5 km depth, the average maximum porosity of material ejected from the aquifer between 0.27 km and 1.5 km depth is 39.7%. There would not have been sufficient porosity in material ejected from the aquifer between the surface and 1.5 km depth to hold the 45% volatile content of the aquifer required to completely fluidize ejecta of a 55 km layered ejecta crater. Therefore, a 0.27 km to 1.5 km depth range of volatiles is considered inconsistent with the full size range of layered ejecta craters.

Figure 5 shows the ratio of deposit volatile content and volatile content of the aquifer, β/Ω, as well as aquifer content, Ω (right Y axis), required to fluidize deposits of 3 to 166 km craters when volatiles are present between 270 meters and 2.5 km. Deposits of 3 km and 4 km craters and deposits of those between 65 and 166 km have ratios of deposit volatile content and aquifer content less than 0.52 and deposits of those craters between 7.5 and 55 km final diameter have ratios of deposit volatile content and aquifer content greater than 0.52. Thus, for any assumed aquifer content, volatile content of deposits of 7.5–55 km craters will be higher than those of deposits of 3 and 4 km craters and 65 to 166 km craters. Assuming that as little as 11% volatiles would have fluidized

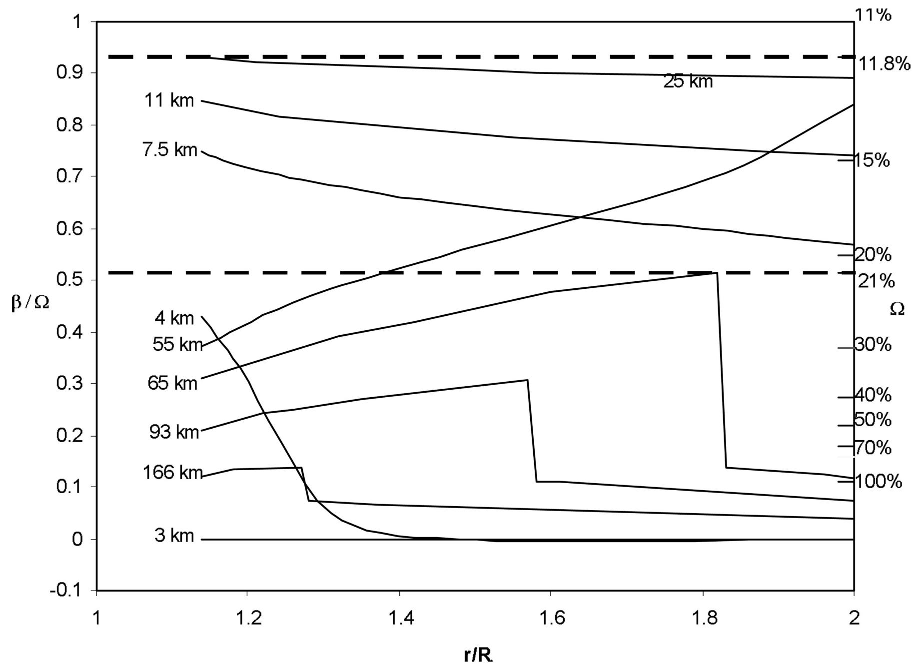

Fig 5. For assumed volatiles between 0.27 and 2.5 km, the graphs show the ratio of percent volatiles in deposits and percent volatiles in the crust (β/Ω) at r/R in deposits (left Y axis) and percent volatiles in the crust (Ω) necessary to fluidized deposits at r/R for craters between 3 and 166 km diameter, assuming 11% volatiles are required to produce fluid flow in crater deposits (right Y axis).

deposits, aquifer content of 11.8%–21% volatiles would have been sufficient to fluidize 7.5 – 55 km crater deposits (Fig. 5.) and 21% aquifer content would not have been sufficient to fluidize deposits of 4 km and smaller craters and those larger than 60 km. Moreover, 21% volatile content is consistent with the maximum permissible porosity of the Martian crust. Assuming the maximum surface porosity of 50%, Equation 16 gives a maximum porosity at 2.5 km depth of 20.6% The average maximum porosity of ejecta from 0.27 km to 2.5 km depth is therefore 35.3%. This exceeds the 21% porosity needed to accommodate the 21% volatiles that would have fluidized deposits of 7.5 km to 55 km diameter craters. Results suggest that 21% volatiles existed between 0.27 km and 2.5 km and this aquifer produced the range in size of layered ejecta craters. Less than 21% volatiles would have failed to fluidize deposits of the largest layered ejecta craters. An aquifer containing more than 21% volatiles is not possible because it would have fluidized deposits of craters larger than 60 km (Fig. 5) that do not have layered deposits.

DISCUSSION

If 11% water/ice caused fluid flow in Martian layered ejecta crater deposits, the observed size range of Martian layered and non-layered ejecta craters in the low and middle latitudes would have been produced if ice/water was present between 270 meters and 2.5 km depth in the crust with concentration of 21% by volume. This volatile content is consistent with an accepted porosity model for the Martian crust. On a global basis, this represents 7.6×10^7 km^3 water/ice between 270 meters and 2.5 km in the Martian crust. Crater size frequency analyses indicate that layered ejecta craters date from the Hesperian and Amazonian periods (Barlow 1990). During Hesperian time, this water/ice would have been available in the crust in the low and middle latitudes. It would have been sufficient to fill a proposed northern lowland ocean (Parker et al. 1989, 1993) to shoreline contact 2 if crustal volatiles supplied water to the outflow channels emptying into the northern lowlands. Head et al. (1999) measured the volume required to fill the northern basins to contact 2 to be 1.4×10^7 km^3 and they proposed that water to fill the basins could have been supplied by the Hesperian outflow channels leading from lower latitudes to the northern lowlands.

The 0.27–2.5 km depth, 21% ice/water aquifer that was derived here from the size range of layered ejecta craters is consistent with the proposed depth and porosity of the Martian megaregolith that could have held the volatiles. A 2–3 km depth has been proposed for this combined porous, ejecta of impact craters that rests on fractured basement rocks (Davis and Golombek 1990). A reasonable surface porosity of 31.8% for the megaregolith would have been compacted with depth to a porosity of 28.9% at 0.27 km depth, 13.1% at the megaregolith-basement interface at 2.5 km depth (Equation 16), and an average porosity of 21%. Results suggest little water in the fractured basement rock beneath the megaregolith. This result is dependant on the size range of layered ejecta craters in most places on Mars that has been assumed here to be 5 to 60 km. While larger layered craters are rare they do exist. If it assumed that craters as large as

65 km exist in most places, model results would permit an aquifer between 0.27 and 3.5 km in most places. This would imply liquid water also exists in the fractured basement rocks.

The ice/water layer concentration predicted from the size range of layered ejecta craters also provides an explanation for the size dependence of different types of Martian layered ejecta craters. SLE and DLE make up 90% percent of layered ejecta craters between 7.5 and 11 km diameter (Barlow and Bradley 1990). β/Ω ratios for deposits of 7.5–11 km craters (Fig. 5) can be used to show that average aquifer ice/water concentration of Ω = 21% would have produced ice/water content of β = 12.4–17.8% in deposits of both SLE and DLE craters of this size. Self-similarity dictates that the size of the continuous deposits of impact craters formed in targets of the same composition (target material and volatile content) should be the same relative to crater size when ejecta is emplaced from low-angle ballistic trajectories and when gravity controls crater growth (Melosh 1989 and Equation 5). Therefore, the inner layers of DLE craters extending, on average, to 2.5 R_f from crater centers (Barlow 2006) and the entire continuous deposits of SLE craters extending, on average, to 2.5 R_f (Barlow 2006) were the deposits that were emplaced by ballistic trajectories followed by ground flow. This is supported by the fact that they extend slightly farther from crater centers than lunar crater deposits (2.35 R_f) that were dry and that were emplaced by ballistic emplacement (Melosh 1989). Low ejecta volatile content and low velocity ground flow produced viscous appearing SLE deposits and viscous appearing inner layer deposits of DLE craters that were only slightly larger than deposits of lunar craters. This finding is consistent with that of Boyce and Mouginis-Mark (2006) who documented straight grooves cut into the inner layers of DLE craters and curved radial lineations on the outer layers of DLE crater deposits and suggested that some non-ballistic high velocity medium scoured the inner layer ejecta of DLE craters from near the rim outward and deposited material in the outer layer after the inner layer was emplaced by ballistic transport and ground surge.

MLE craters become dominant at 25 km (Barlow and Bradley 1990). β/Ω ratios for 25 km craters given in Fig. 5 (.9–.95) show that average water/ice content of Ω = 21% in the aquifer would have produced β = 19–20% water/ice in MLE crater deposits, a higher concentration than for the smaller SLE and DLE crater deposits. The reason for the higher water/ice content is that depth of excavation of the 25 km MLE craters lies almost entirely within the typical 0.27–2.5 km aquifer (See also Fig. 12 of Barlow and Bradley [1990] showing MLE craters forming mostly in the volatile rich layer) whereas significant fractions of the excavation volumes of smaller SLE, DLE craters were found here to be outside the aquifer. The higher water content and ground surge velocity of the ejecta ground surge of MLE craters produced a more mobile and larger but thinner continuous deposits for MLE craters. They extend, on average 3.17 R_f from crater centers (Barlow 2006). Higher deposit volatile composition and self-similarity permitted larger deposits than for smaller SLE and DLE craters.

MLE make up a lower percentage of layered ejecta craters larger than 25 km. SLE craters and craters having some fluid structures and some features resembling lunar crater deposits (diverse craters) combined are dominant above 40 km (Barlow and Bradley 1990). β/Ω ratios are from 0.52–0.85 for deposits of 55 km craters (Fig. 5) indicating, for a 21% volatile aquifer, a deposit water/ice content of 11% to 17.8% for 55 km crater deposits, about equal to the ice/water content of 7.5–11 km SLE crater deposits. Thus, deposits of small and large SLE craters and large diverse craters have similar and low ranges in volatile content because large SLE and diverse craters eject about equal fractions of ejecta from above and below the aquifer as small SLE craters eject from above the aquifer. This accounts for the presence of SLE craters and diverse craters above 40 km and the dominance of SLE craters below 25 km.

Previously, the change in morphology of Martian layered ejecta crater deposits with crater size has been related to the change in state of water with depth relative to the depth of penetration of the crater, excavation to depths near the volatile poor-volatile rich boundary, and the presence or absence of ice/water determined by the depth of excavation of the crater. Barlow and Bradley (1990) hypothesized that radial craters greater than 64 km, similar to lunar craters, formed because they excavated in volatile poor regions at greater than 4.34 km depth. 8–20 km SLE craters were believed to be dominant below 20 km because they sampled near surface ice between 0.75–1.63 km depth but MLE craters between 16 km and 45 km formed because they excavated into brines between 1.35 km and 3.24 km. Results presented here are consistent with the presence of near surface ice and liquid water at depth but considerations of streamlines for crater excavation point to ejecta deposit volatile concentration as important for determining the type of layered ejecta crater that forms.

Layered ejecta craters smaller than 5 km and larger than 60 km do not exist in most places in the low and middle latitudes of Mars. Crater deposits resemble those of lunar craters. β/Ω ratios in Fig. 5 are less than 0.52 for deposits of craters smaller than 5 km and larger than 60 km. For Ω = 21% volatiles in the crust containing volatiles, there would have been less than 11% water in deposits of these craters, an amount not sufficient to produce fluid flow. The dry crust above 0.27 km and below 2.5 km makes up such a large fraction of the craters of excavation of craters smaller than 5 km and larger than 60 km, respectively, that there was not enough water/ice in the ejecta to fluidize crater deposits. In addition, ballistic erosion occurred only for deposits of craters larger than 60 km that incorporated very large amounts of dry near surface material into deposits. Thus, while ballistic erosion acted on Mars to reduce deposit fluidization for craters larger than 60 km, it would have produced fluidization in deposits of terrestrial craters larger than 25 km like those of the Ries crater if near surface volatiles were present.

In places, ice/water must have been present at shallower depths than 0.27 km on Mars because layered ejecta craters smaller than 5 km occur in those regions. Reiss et. al. (2006) and Demura and Kurita (1998) reported layered ejecta craters less than 1.5 km in the east edge of Chryse Planitia. Barlow et al. (2001) reported layered ejecta crater onset diameters less than 5 km in the Solis and Thaumasia Planum regions. For this reason, provided that ground surge velocity was high enough, a higher percentage of small MLE craters might exist where volatiles were present near the surface than in most of the low and mid-latitude regions.

Results presented here suggest that outer upper layers of DLE craters cannot be explained by ground surge caused by ballistic impact of crater ejecta. Boyce and Mouginis-Mark (2006) hypothesized that either ground flow occurred from crater rim outward in a non-ballistic emplacement phase similar to a volcanic base surge or atmospheric interaction with the ejecta curtain produced outer layers. Osinski (2006) suggested that volatile rich impact melts formed outer upper layers of DLE crater deposits on top of ballistic ejecta. Formation of outer upper layers of DLE craters from atmospheric drag on ejecta and the presence of SLE and DLE craters near one another require that craters formed at times when atmospheric pressure was different. Base surges require a near vertical ejection curtain from high angle ejection to feed the base surge over prolonged time near the crater rim so that the base surge could have eroded the top of the inner layer, that was deposited first. Vertical ejection columns exist for impacts in water. If DLE craters formed in shallow surface water, a vertical ejection column from the surface may have produced a base surge following 45° angle deeper ejecta that formed the inner layers of DLE crater deposits. However, this explanation also requires frequent changes in atmospheric pressure to account for periods where surface water would have been stable. Still other mechanisms might explain outer layer deposits of DLE craters. For example, target layering can produce bimodal ejection angles so that high angle ejection from the substrate can deposit material on low angle surface ejecta.

The values for ratios of deposit volatile content and crustal volatile content for layered ejecta crater deposits and the resulting crustal volatile content that have been obtained in this paper resulted from a series of linked calculations using equations with many variables. These parameters include the k value in Equation 2, that depends on target porosity, the exponent in $(r_c/R)^{-1.8}$ in Equation 2 that ranges from −1.5, −1.8, and −2.4 for impacts in basalt, water, and quartz sand respectively, ejection angle, constants in Equation 9b for L, onset of ballistic erosion velocity, and the value of Z assumed for the Z model. Later studies assuming different values reflecting uncertainties for these parameters can be performed to generate error bars for volatile concentration and distribution in the crust. For example, lowering the onset velocity for ballistic erosion to 200 m/s would reduce the volatiles in deposits of 65 km and 93 km craters and permit a deeper aquifer. However, the successful prediction of the size distribution of layered ejecta craters from an aquifer consistent with the porosity of the Martian crust suggests that volatiles are probably responsible for fluidization of deposits.

Estimates of volatile contents could be revised if crater deposit scale affects the amount of water/ice needed to fluidize crater deposits. An ejecta emplacement Bingham model for Martian crater deposit emplacement gives model parameters that are between those for dry flows and volatile rich debris flows and it provides a potential methodology for estimating volatile content of deposits (Ivanov 1996; Ivanov and Pogoretsky 1996; Ivanov et al. 1997). Deposit scale was found to affect the extent of flow of Martian impact crater deposit material relative to crater size and it has been suggested that this is due to scale dependent flow characteristics. This suggests the possibility that large crater deposits might require less water to fluidize crater deposits than small ones. In this event, scale dependent percentages of volatiles needed for deposit fluidization could be applied to ratios of β/Ω found here for deposits of different size craters to derive lower volatile content for the aquifer.

What if more than 11% water/ice was required to fluidize Martian crater deposits? If as much as 18% water/ice was required to produce fluid flow in crater deposits, volatiles would still be viable for fluidizing crater deposits. β/Ω ratios in Fig. 5 are as small as 0.52 for the layered ejecta craters. Thus, an aquifer water/ice percentage (Ω) as high as 34.6 % would have been required to produce a value as large as 18% and fluidize these deposits where β/Ω can be as small as 0.52. The average porosity of 35% between 270 meters and 2.5 km would have been sufficient to contain 34.6% volatiles in the crust. If more than 18% was required to fluidize deposits, the β/Ω ratios of deposits of 55 km craters would require more than 35% volatiles in the aquifer to fluidize all of the deposits of layered ejecta craters. The porosity of the crust would not have been sufficient to hold this amount of water. In this case volatiles would not have been effective agents for deposit fluidization of the full size range of layered ejecta craters.

Cockell and Barlow (2002) suggested that Martian ejecta blankets might be good sites to search for evidence of life-forms. During Hesperian and Amazonian time layered ejecta craters were present between 5 km and 60 km in most regions in the low and middle latitudes suggesting that ice/water existed deeper than 270 meters. In places volatiles must have been present at shallower depths than 270 m because layered ejecta craters much smaller than 5 km have been discovered in the equatorial regions (Reiss et. al. 2006) and Demura and Kurita (1998) reported layered ejecta craters less than 1.5 km in the east edge of Chryse Planitia. Barlow et al. (2001) reported such SLE crater onset diameters in the Solis Planum and Thaumasia Planum regions. At earlier times in Martian history before most of the layered ejecta craters formed, water was likely present at or very near the surface and global sterilizing impacts would have ended, thus permitting conditions suitable for the origin of life (Oberbeck and Fogleman 1990). Organisms could have migrated to the subsurface with the receding water table and organisms or fossils would have been ejected from layered ejecta craters that formed later.

Deposits of Martian layered ejecta craters may be ideal sites to search for fossils of primitive organisms on Mars because the turbulence occurring during the ground surge of deposit emplacement would have distributed them uniformly in deposits. For example, the Devonian Alamo impact, Nevada, occurred in shallow water and the crater excavated pre-Devonian conodont fossils at pre-impact horizons in pre-Devonian strata and mixed them uniformly into the fluidized deposits of the Alamo impact deposit (Morrow et al. 1998). Searches for fossils of organisms in deposits of Martian ejecta craters might be aided by the fact that organisms living in the deep water table or fossils would have been excavated and they would have been mixed uniformly into the fluidized deposits during deposit emplacement as they were for the Alamo impact deposit. Random samples might yield samples of microscopic fossils. On the other hand, search for fossils in isolated stratigraphic positions in Martian rock formations may be much more difficult because only limited vertical horizons are typically fossil rich in terrestrial formations.

CONCLUSION

The size distribution of Martian layered ejecta craters and the change in the type of layered ejecta crater with size is entirely consistent with the ballistic sedimentation of primary crater ejecta as for lunar craters, but volatiles in ejecta account for the different appearance of Martian crater deposits. In this paper, an impact Z model for excavation of material from the Martian crust has been used together with an ejection model for impact craters whose growth is controlled by gravity to determine the percentage of volatiles in the streamlines of crater excavation and the range of impact of this ejecta in the crater deposit. The extent of erosion of the surface area outside the crater by the impacting ejecta was evaluated and used to determine, with the percentage of volatiles in the ejecta, the ratio of percentage of volatiles in the deposit and the percentage of volatiles in the aquifer at any location where ejecta impacted outside the crater. The percentage of volatiles needed to fluidize debris flows in terrestrial debris flows was used with these ratios to determine the depth of the aquifer and percentage of volatiles in the Martian crust that was consistent with the size range of layered ejecta craters. The observed size range of craters could only be produced if volatiles were present between 0.27 and 2.5 km depth at a concentration of 21% during Hesperian and Amazonian time. This would have been more than enough to fill a northern lowland ocean from Hesperian outflow channels draining some of the highlands megaregolith to the south. This would seem to indicate loss of some of the volatile inventory at middle and low latitudes to the northern lowlands and eventually to space. The 0.27–2.5 km ice/water-rich layer early in history is consistent with the 2–3 km depth of the Martian megaregolith and a previously published model for porosity of the Martian megaregolith. The depth of the aquifer and its volatile concentration is also consistent with the change in the type of layered ejecta crater with size and with the absence of layered ejecta craters for the size ranges observed on Mars. Finally, these results, suggesting that ice/water fluidized layered ejecta craters, point to the layered ejecta deposits as prime sites to search for evidence of past life on Mars.

Acknowledgments—I thank Friedrich Hörz for his useful comments and interest in the early phase of this work. Nadine Barlow provided useful and insightful comments in the detailed reviews of the work. I thank Boris Ivanov for his helpful review and for drawing my attention to scale effects on crater deposit fluidization, and the Martian crustal porosity depth profile, and for other helpful suggestions. An early review by Peter Mouginis-Mark is acknowledged.

Editorial Handling—Dr. Uwe Reimold

REFERENCES

Barlow N. G. 1990. Constraints on early events in Martian history as derived from the cratering record. *Journal of Geophysical Research* 95:14191–14201.

Barlow N. G., Koeshetz J., and Dohm J. M. 2001. Variations in the onset diameter for Martian layered ejecta morphology morphologies and their implications for subsurface volatile reservoirs. *Geophysical Research Letters* 28:3095–3098.

Barlow N. G. and Bradley T. L. 1990. Martian impact craters: Correlations of ejecta and interior morphologies with diameter, latitude and terrain. *Icarus* 87:156–179.

Barlow N. G. 2006. Martian impact craters and their implications for target characteristics. Proceedings, First International Conference on Impact Cratering in the Solar System. ESTEC Special Publication 612. pp. 17–25.

Barnouin-Jha O. S. and Buczkowski D. L. 2007. Comparing the runout distances of fluidized ejecta on Mars with mass movements on Earth (abstract #1304). 38th Lunar and Planetary Science Conference. CD-ROM.

Barnouin-Jha O. S. and Schultz P. H. 1998. Lobateness of impact ejecta deposits from atmospheric interactions. *Journal of Geophysical Research* 103 E11:25,739–25,756.

Barnouin-Jha O. S., Schultz P. H., and Lever J. H. 1999 Investigating the interactions between an atmosphere and an ejecta curtain. *Journal of Geophysical Research* 104:27,117–27,132.

Barnouin-Jha, Baloga S., and Glaze L. 2005. Comparing landslides to fluidized crater eject on Mars. *Journal of Geophysical Research* 110:E04010, doi:10.1029/2003JE002214.

Boyce J. M. and Mouginis-Mark P. 2006. Martian craters viewed by the Thermal Emission Imaging System Instrument: Double-layered ejecta craters. *Journal of Geophysical Research* 111: E10005, doi:10.1029/2005JE002638.

Carr M. H. 1977. Distribution and emplacement of ejecta around Martian impact craters. In: *Impact and explosion cratering*, edited by Roddy D. J., Pepin R. O., and Merrill R. B. New York: Pergamon Press. pp. 593–602.

Carr M. H., Crumpler L S., Cutts J. A., Greeley R., Guest J. E., and Masursky H. 1977. Martian impact craters and emplacement of ejecta by surface flow. *Journal of Geophysical Research* 82: 4055–4065.

Cintala M. J., Berthoud L., and Hörz F. 1999. Ejection-velocity distributions from impacts in coarse-grained sand. *Meteoritics & Planetary Science* 34:605–623.

Clifford S. M. 1993. A model for the hydrologic and climatic behavior of water on Mars. *Journal of Geophysical Research* 98: 10,973–11,016.

Cockell C.S. and Barlow N. G. 2002. Impact excavation and the search for subsurface life on Mars. *Icarus* 155:340–349.

Collins G. S., Melosh H. J., and Marcus R. A. 2005. Earth impact effects program: A web-based computer program for calculating the regional environmental consequences of a meteoroid impact on Earth. *Meteoritics & Planetary Science* 40:817–849.

Croft S. K. 1980. Cratering flow fields: Implications for the excavation and transient expansion stages of crater formation. Proceedings, 11th Lunar and Planetary Science Conference. pp. 2347–2378.

Davis P. A. and Golombek M. P. 1990. Discontinuities in the shallow Martian crust at Lunae Syria and Sinai Plana. *Journal of Geophysical Research* 95:14,231–14,298.

Demura H. and Kurita K. 1998. A shallow volatile layer at Chryse Planitia, Mars. *Earth, Planets and Space* 50:423–429.

Fink J. H., Greeley R., and Gault D. E. 1981. Impact cratering experiments in Bingham materials and the morphology of craters on Mars and Ganymede. Proceedings, 12th Lunar and Planetary Science Conference. pp. 1649–1666.

Gault D. E. and Greeley R. 1978. Exploratory experiments of impact craters formed in viscous-liquid targets: Analogs for Martian rampart craters? *Icarus* 34:486–495.

Greeley R. J., Fink J. H., Gault D. E., Snyder D. B. Guest J. E., and Schultz P. H. 1980. Impact cratering in viscous-liquid targets: Laboratory experiments. Proceedings, 11th Lunar and Planetary Science Conference. pp. 2075–2097.

Head J. W. and Roth W. R. 1976. Mars pedestal crater escarpments: Evidence for ejecta related emplacement: In: *Symposium on planetary cratering mechanics*. Houston: Lunar and Planetary Institute. pp. 50–52.

Head J. W. III., Hiesinger H., Ivanov M. A., Kreslavsky M. A., Pratt S., and Bradley J. T. 1999. Possible ancient oceans on Mars: Evidence from Mars Orbiter Laser Altimeter data. *Science* 286:2134–2137.

Hörz F., Gall H., Huttner R., and Oberbeck V. R. 1977. Shallow drilling in the 'Bunte Breccia' impact deposits, Ries Crater, Germany. In *Impact and explosion cratering*, edited by Roddy D. J., Pepin R. O., and Merrill R. B. New York: Pergamon Press. pp. 425–448.

Hörz F., Ostertag R., and Rainey D. A. 1983. Bunte Breccia of the Ries: Continuous deposits of large impact craters. *Reviews of Geophysics and Space Physics* 84:7669–7687.

Housen K. R., Schmidt R. M., and Holsapple K. A. 1983. Crater ejecta scaling laws: Fundamental forms based on dimensional analysis. *Journal of Geophysical Research* 88:2485–2499.

Ivanov B. A. 1996. Spread of ejecta from impact craters and the possibility of estimating the volatile content of the Martian crust. *Solar System Research* 30:36–50.

Ivanov B. A. and Pogoretsky A. V. 1996. Bingham parameters for fluidized ejecta spreading on Mars and Martian volatiles (abstract #1587). 27th Lunar and Planetary Science Conference.

Ivanov B. A., Pogoretsky A. V., and Murray B. 1997. Fluidized ejecta blankets on Mars: Estimate of material properties. 28th Lunar Planetary Science Conference. pp. 637–638.

Kuzmin R. O., Bobina N.l N., Zabalueva E. V., and Shashkina V. P. 1988. Structural inhomogeneities of the Martian cryolithosphere. *Solar System Research* 22:121–133.

McGetchin T. R., Settle M., and Head J. W. 1977. Radial variations in impact crater ejecta: Implications for lunar basin deposits. *Earth and Planetary Science Letters* 20:226–236.

McSaveney M. J. and Davies T. R. H. 2005. Making a land bridge connection between two rocky planets. *Workshop on Role of Volatiles and Atmospheres on Martian Impact Craters*. LPI Contribution 1273. Houston: Lunar and Planetary Institute. pp. 73–74.

Melosh H. J. 1989. *Impact cratering: A geologic process*. New York: Oxford University Press. 245 p.

Morrison R. H. and Oberbeck V. R. 1978. A comparison and thickness model for lunar impact crater and basin deposits. Proceedings, 9th Lunar and Planetary Science Conference. pp. 3763–3785.

Morrow J. R., Sandberg C. A., Warme J. E., and Kuener H. 1998. Regional and possible global effects of sub-critical late Devonian Alamo impact event, southern Nevada, USA. *Journal of The British Interplanetary Society* 51:451–460.

Mouginis-Mark P. J. 1981. Ejecta emplacement and modes of formation of Martian fluidized ejecta craters. *Icarus* 45:60–76.

Oberbeck V. R. 1975. The role of ballistic erosion and sedimentation in lunar stratigraphy. *Reviews of Geophysics and Space Physics* 13:337–362.

Oberbeck V. R. and Fogleman G. 1990. On the possibility of life on early Mars. Proceedings, 20th Lunar and Planetary Science Conference. pp. 473–478.

Osinski G. R. 2006. Effect of volatiles and target lithology on the generation and emplacement of impact crater fill and ejecta deposits on Mars. *Meteoritics & Planetary Science* 41:1571–1586.

Parker T. J., Saunders R. S., and Schneeberger D. M. 1989. Transitional morphology in west Deuteronilus Mensae, Mars: Implications for modification of the lowland/upland boundary. *Icarus* 82:111–145.

Parker T. J., Gorsline D. S., Saunders R. S., Pieri D. C., and Schneeberger D. M. 1993. Coastal geomorphology of the Martian northern plains. *Journal of Geophysical Research* 98: 11,061–11,078.

Petro N. E. and Pieters C. M. 2006. Modeling the provenance of the Apollo 16 regolith. *Journal of Geophysical Research* 111: E09005, doi: 10.1029/2005JE002559.

Pierson T. C. 1980. Erosion and deposition by debris flows at Mt. Thomas, North Canterbury, New Zealand. *Earth Surface Processes* 5:227–247.

Riess D., Van Gasselt S., Hauber E., Michael G., Jaumann R., and Neukum G. 2006. Ages of rampart craters in equatorial regions on Mars: Implications for the past and present distribution of ground ice. *Meteoritics & Planetary Science* 41:1437–1452.

Rodine J. D. and Johnson A. M. 1976. The ability of debris, heavily freighted with coarse clastic materials, to flow on gentle slopes. *Sedimentology* 23:213–234.

Schultz P. H. 1992. Atmospheric effects on ejecta emplacement. *Journal of Geophysical Research* 97(E7):11,623–11,662.

Schultz P. H. and Gault D. E. 1979. Atmospheric effects on Martian ejecta emplacement. *Journal of Geophysical Research* 84:7669–7687.

Stewart S. and Ahrens T. 2003. Shock Hugoniot of H_20 ice. *Geophysical Research Letters* 30:1332.